Ore Geology Reviews 161 (2023) 105628

Contents lists available at ScienceDirect

Ore Geology Reviews

journal homepage: www.elsevier.com/locate/oregeorev

LA–ICP–MS analysis of sulfides from the Jianzhupo deposit, Guangxi Province, China: Insights into element incorporation mechanisms and ore genesis

Yunzhu Wu [a,b], Zhen Yang [b], Chuang Zhou [b], Lisheng Gao [a], Wenrui Song [a,b], Qiankun Li [a], Yuxu Zhang [a], Hanjie Wen [c,d], Chuanwei Zhu [a,*]

[a] State Key Laboratory of Ore Deposit Geochemistry, Institute of Geochemistry, Chinese Academy of Sciences, Guiyang 550081, China
[b] School of Earth Resources, China University of Geosciences, Wuhan 430074, China
[c] School of Earth Sciences and Resources, Chang'An University, Xi'an 710054, China
[d] College of Earth and Planetary Sciences, University of Chinese Academy of Sciences, Beijing 100049, China

ARTICLE INFO

Keywords:
Jianzhupo deposit
LA–ICP–MS
Trace element
Sphalerite
Jamesonite
Stibnite

ABSTRACT

The Jianzhupo deposit, the largest Zn-Sb deposit in the Wuxu orefield in China, contains abundant sphalerite and jamesonite, contrasting with typical Sb deposits elsewhere. Whether the Sb and Zn in the deposit derived from similar parental sources is not clearly resolved. Here, trace-element compositions of sulfides from the deposit were determined by laser ablation–inductively coupled plasma–mass spectrometry (LA-ICP-MS). Results indicate that jamesonite is an important Cd-bearing sulfide with Cd contents of 523–764 ppm and minor or no significant Cd variations were observed within jamesonite crystals. Trace-element compositions of jamesonite indicates that Cd enters the lattice by coupled substitution as $2Fe^{2+} \leftrightarrow Zn^{2+} + Cd^{2+}$. Due to similar geochemical behaviors between Zn and Cd in hydrothermal systems, Zn/Cd ratio of sphalerite was suggested as a robust geochemical tracer to distinguish metal sources in such systems. Here, we summarized the Zn/Cd ratios of sphalerite from various hydrothermal systems and the results show that values between 169 and 233, and lower than 44 are from high- and low-temperature temperature fluid conditions, respectively. Due to different Zn/Cd ratios between sediments and igneous rocks, we conclude that metals in sphalerite from the Jianzhupo deposit were likely derived from granite; in contrast, metals in jamesonite were related to sedimentary rocks. These conclusions are consistent with previous studies on the deposit. Overall, our results indicate that ore-forming fluids of the Jianzhupo deposit were derived from magmatic–hydrothermal and basin water. This study extends the application of trace-element compositions in resolving the sources of sulfides in hydrothermal systems.

1. Introduction

The Jianzhupo deposit is located in the Wuxu orefield in Guangxi Province, China, in the southeastern Danchi metallogenic belt, which is well known as a non-ferrous metal production area with several large-scale deposits such as the Dachang Zn–Sn–Sb–In deposit (Fig. 1; Cai et al., 2012; Liu et al., 2015). Pb–Zn–Sb polymetallic deposits are concentrated in the middle of the Wuxu orefield, while those in the north and southeast are mainly Hg deposits formed under low-temperature conditions (Fig. 1C).

Due to the lack of exposed granite in the study area, the genesis of ore deposits in the Wuxu orefield is not well constrained. Thus, tracing their metal sources and analyzing metal combinations would improve our understanding of metallic mineralization and guide anamineral exploration. As the largest deposit in the Wuxu field, the Jianzhupo deposit has been studied in terms of S isotopes, bulk trace element compositions of sphalerite, H–O isotopes, and fluid inclusions (Zhang et al., 2018a, b; Liu et al., 2020), but the source of ore-forming fluids is debated. Based on S isotopes and trace elements in sphalerite, the fluids may be mainly of magmatic–hydrothermal origin (Liu et al., 2020; Xiao, 2022); however, H–O isotopic compositions of fluid inclusions indicate an origin from both magmatic–hydrothermal and basin waters (Zhang et al., 2018 a, b). Recently, Cd isotope signatures of sphalerite and jamesonite are different, and the results also support that metals from the deposit were

* Corresponding author.
E-mail address: zhuchuanwei@mail.gyig.ac.cn (C. Zhu).

https://doi.org/10.1016/j.oregeorev.2023.105628
Received 27 April 2023; Received in revised form 16 August 2023; Accepted 19 August 2023
Available online 21 August 2023

derived from mixture of igneous and sedimentary rocks (Yang et al., 2023).

LA–ICP–MS is useful in determining the geochemical compositions of minerals formed in various types of hydrothermal systems, and has been widely applied in analyzing sulfides to trace mineralization conditions and deposit genesis, and in the classification of hydrothermal systems (Cook et al., 2009; Ye et al., 2011; Wei et al., 2018; Li et al., 2019a, 2019b; Hu et al., 2020; Li et al., 2021; Liu et al., 2022). For example, sphalerite from different types of deposit has characteristic patterns of trace-element enrichment: Mississippi Valley type (MVT) deposits are enriched in Ge, Cd, and Ga; epithermal deposits in As, Ag, Sb, and Mo; skarn deposits in Mo and Co; and volcanogenic massive sulfide (VMS) and sedimentary exhalative (SEDEX) deposits in Mn, Fe, and In (Cook et al., 2009; Li et al., 2020). Deposit types have also been classified by comparison of binary plots of trace elements in sulfides (Ye et al., 2011; Hu et al., 2021). By comparing the trace element composition of stibnite from different types of Sb deposits, the deposit type can be effectively determined (Fu et al., 2020; Song et al., 2022; Zhou et al., 2023). Such as, Fu et al. (2020) found that the Hg / (Cu + Pb) ratio of the Xikuangshan deposit is greater than 1 and metals from this deposit are dominantly derived from basements; in contrast, the Woxi deposit is lower than 1 and basements were not likely provided metals to the deposit. Such studies have established that geochemical compositions of sulfides may record information on ore-forming processes in Sb deposits.

Here, LA–ICP–MS was applied in determining the major- and trace-element compositions of sphalerite, jamesonite, and stibnite in the Jianzhupo deposit. Based on the correlations between elemental concentrations, we investigated enrichment mechanisms of major and trace elements, and discuss metal sources of the deposit by comparing various elemental enrichment signatures in different types of hydrothermal systems.

2. Geological setting

2.1. Regional geology

The Wuxu, Mangchang, and Dachang orefields form the main framework of the Danchi metallogenic belt (Fig. 1B; Xiao, 2018), lying on the outer southwestern margin of the Jiangnan Massif and the northeastern margin of the Youjiang Basin (Fig. 1B) at the intersection of the Paleo-Tethyan and Paleo-Pacific tectonic domains (Zhao and Liu, 2016; Xu et al., 2019). Geological events provided favorable conditions for the formation of Pb–Zn–Sb deposits (Fig. 1A, B; Fu et al., 1993; Cai et al., 2007; Xiao et al., 2022a). Devonian, Carboniferous, Permian, and Triassic strata are exposed in the Wuxu orefield (Fig. 1C). Devonian strata contain the main host rocks of polymetallic deposits, mainly mudstone, marlstone, siliceous rocks, and limestone (Zhang et al., 2018a, b). Carboniferous strata comprise mainly mudstone, limestone, and dolomite; Permian strata limestone, marlstone, and siliceous rock; and Triassic strata mudstone, shale, limestone, siltstone, and siliceous rock (Zhang et al., 2018a, b; Xiao, 2018).

NNW-trending folds and transtensional faults constitute the main structural framework of the Wuxu orefield. E–W-trending faults were formed through torsion of the NNW-trending faults, which cut second-stage NNE-trending faults that formed during late tectonic activity (Fig. 1C; Liu et al., 2020; Xiao, 2018). Magmatic rocks are exposed in the Mangchang and Dachang orefields, but not in the Wuxu orefield (Fig. 1B; Liang et al., 2011; Zhao et al., 2018). Negative gravity

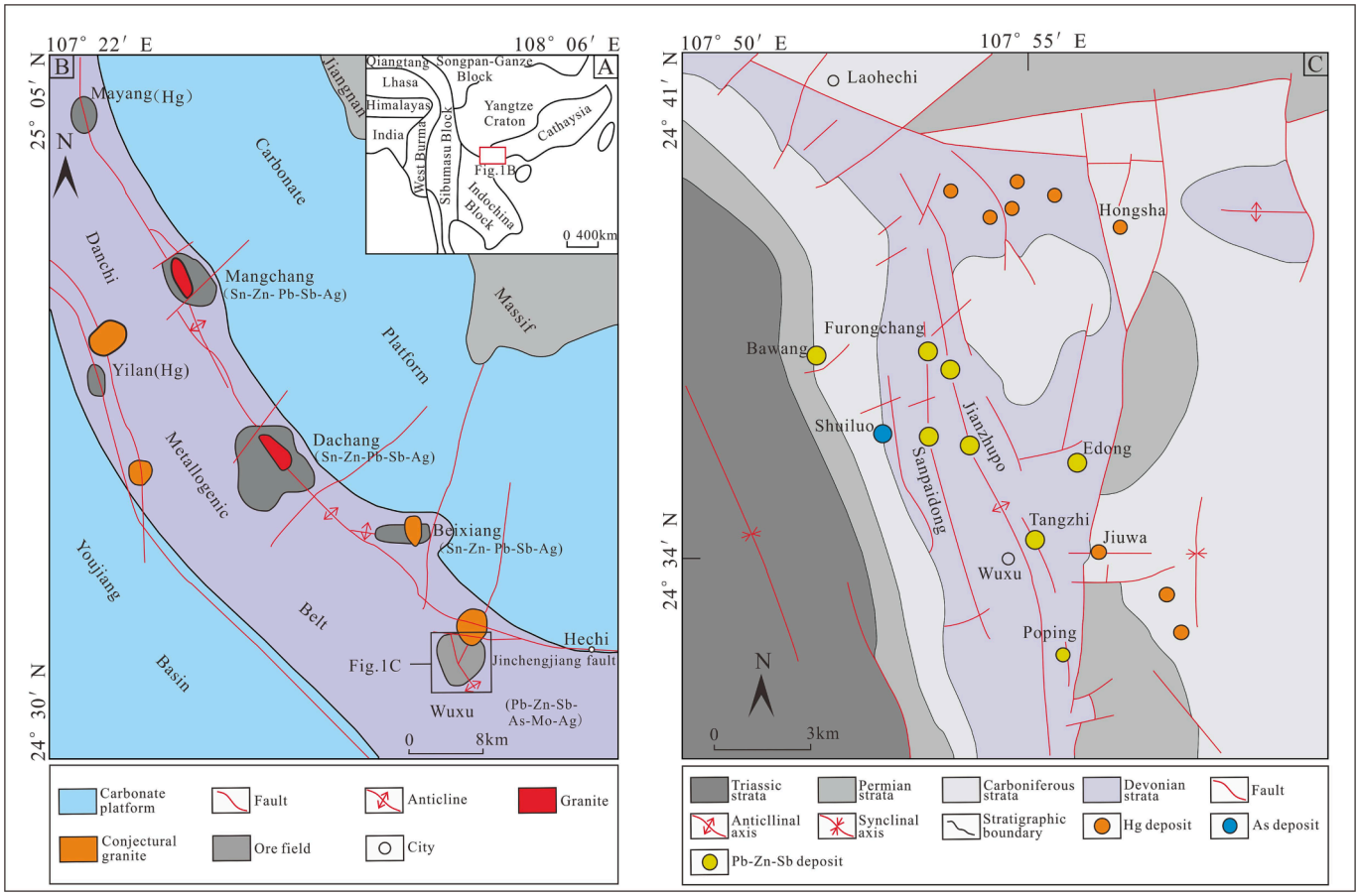

Fig. 1. (A) Tectonic sketch map; (B) Geological sketch map of the Danchi polymetallic ore belt (after Cai et al., 2012); (C) Geological map of the Wuxu ore field (after Cai et al., 1995). Granites in Dachang mainly consist of biotite granites (the Longxianggai pluton) and granite/diorite porphyry dykes (Guo et al., 2018); Magmatic rocks exposed in Mangchang are grain granites and porphyritic granites, and their related granite dykes (Wu et al., 2020).

anomalies indicate that unexplored granite is likely existed in the middle of the Wuxu orefield (Fig. 1C; Sun et al., 1994).

2.2. Deposit geology

The Jianzhupo deposit is the largest Pb–Zn–Sb polymetallic deposit in the Wuxu orefield (Zhang et al., 2018a, b; Xiao, 2022). The main exposed strata in the field are from the Tangding Formation, which is subdivided into three units based on lithology: Unit 1 comprises mainly mudstone and siltstone; Unit 2 mudstone, marlstone, and silty mudstone; and Unit 3 mudstone and silty mudstone (Chang et al., 2016; Xiao et al., 2022a, b). Faults in the mining area are predominantly NNW-trending transtensional faults and NNE-trending torsional faults. The former are consistent with the trend of orebodies and are the main ore-controlling structures (Fig. 2A; Xiao, 2018).

In Unit 2, orebodies trend NNW and occur mainly in vein, strip, and lenticular forms, with their size and shape controlled mainly by NNW-trending faults (Fig. 2 A, B; Hu et al., 2017; Xiao, 2018). More than 130 veins have been identified in the Jianzhupo deposit, with the main veins being J1, J3, J6, J7, J9, J10, J13, J30, J33, and J59, which together contain large metal reserves (Zhao and Liu, 2016). The economic minerals are predominantly sphalerite and jamesonite with minor pyrite, stibnite and galena, together accounting for > 90% of the total economic minerals. Gangue minerals include quartz, calcite, and sericite (Zhang et al., 2018a, b). Based on field observations, the ores can be divided into two types, including the massive and veined ores (Yang et al., 2023). As the two predominant economic minerals in the deposit, sphalerite is closely associated with jamesonite, and sphalerite is commonly crossed by needle-like jamesonite. Sphalerite has colors varying from black to light, and is mainly subhedral to anhedral. (Fig. 6A). Jamesonite is present as needle-like or spotted crystals in sphalerite (Fig. 3A, B).

Field and optical microscopy observations (Fig. 3) indicate three metallogenic stages: (I) a quartz–pyrite stage that produced mainly pyrite; (II) a quartz–cassiterite sulfide stage that produced large amounts of sphalerite, jamesonite, galena, and stibnite; and (III) a quartz–carbonate stibnite stage that produced mainly carbonate minerals and minor stibnite (Liu et al., 2020; Xiao et al., 2021).

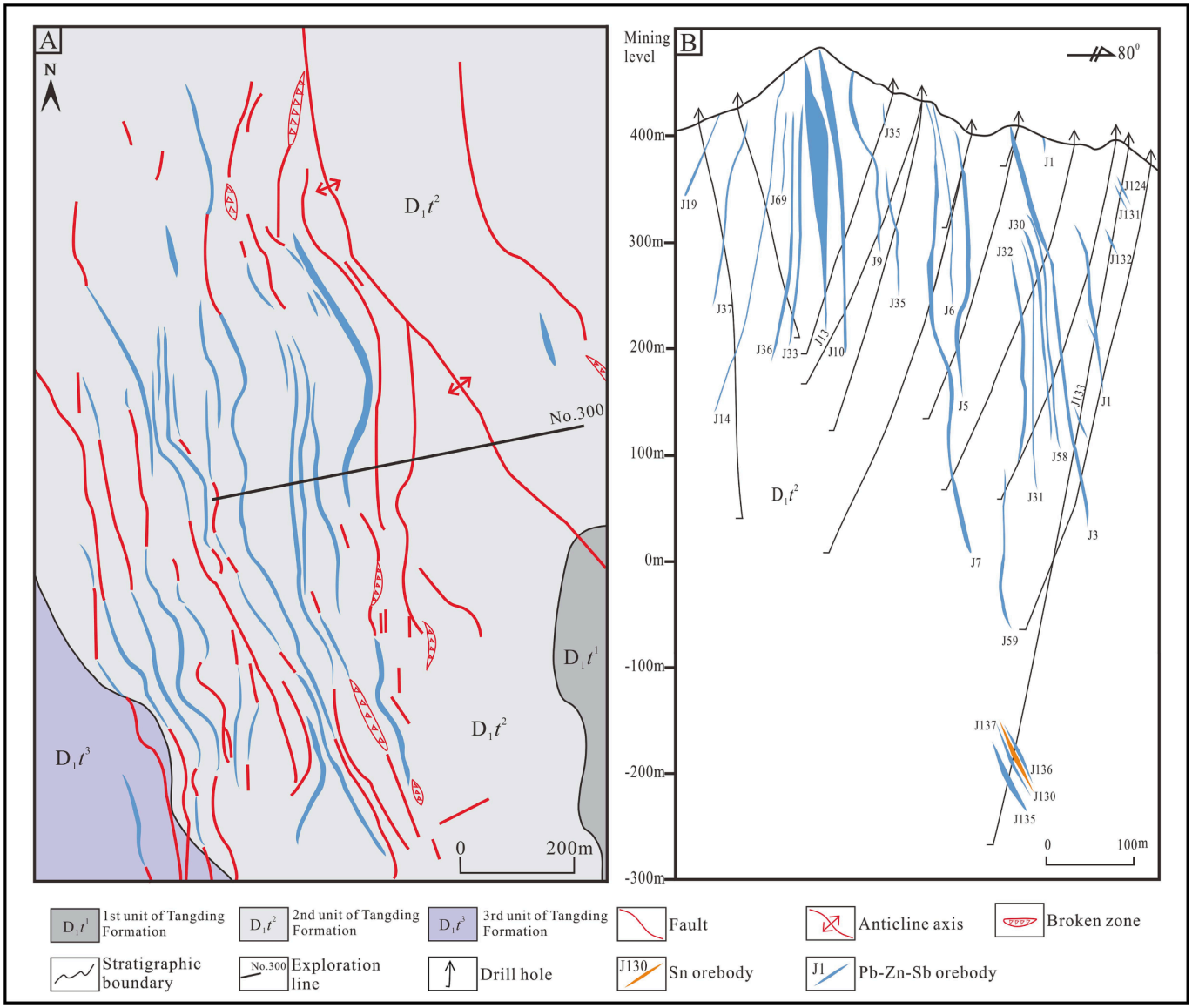

Fig. 2. Geological sketch map (A; modified from Wang, 2012) and cross-section along the No. 300 exploration line (B; modified from Cai et al., 1995) of the Jiangzhupo deposit.

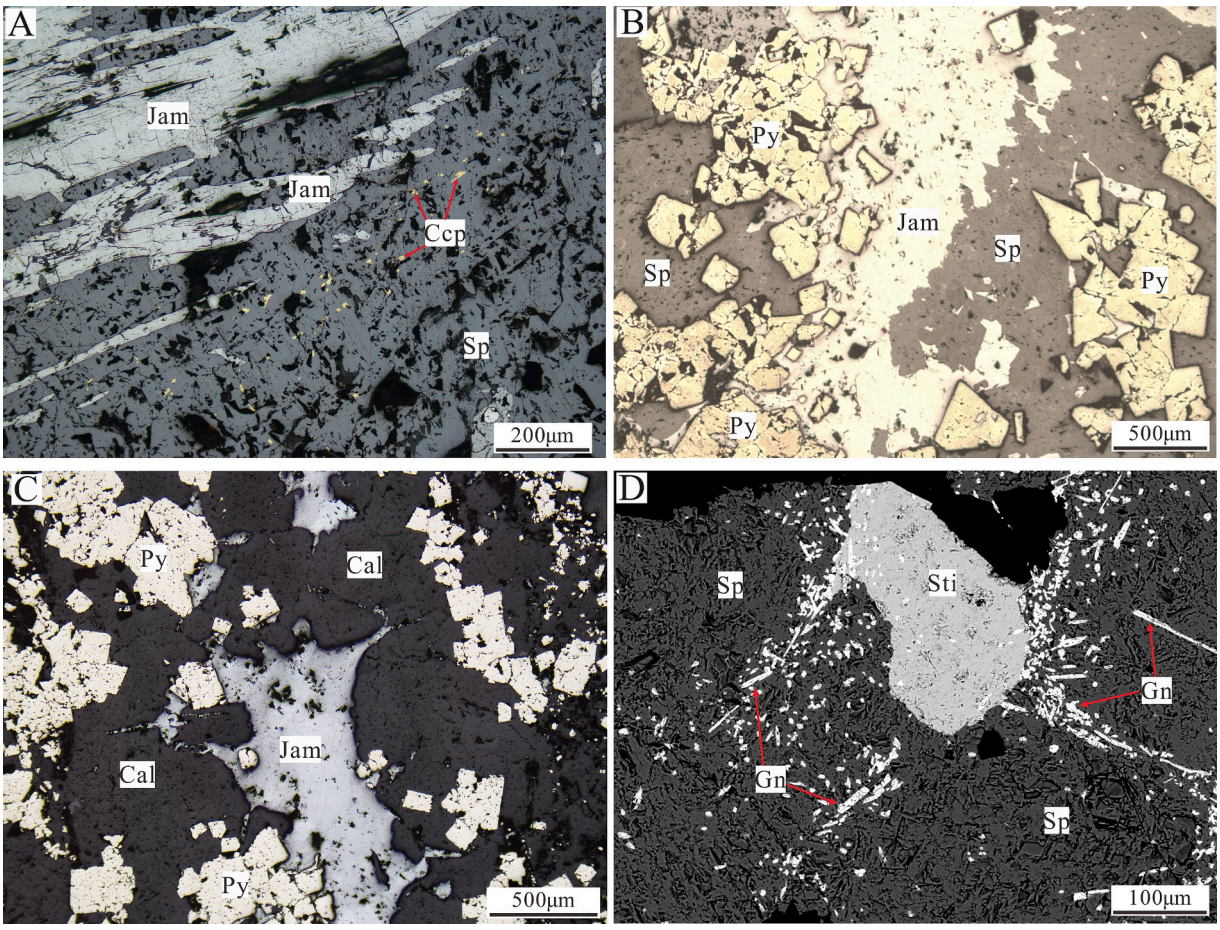

Fig. 3. Photographs of the sulfide ores from the Jianzhupo deposit. (A) Sphalerite with chalcopyrite micro-inclusions crosscut by needle-like jamesonite. (B) Pyrite crystal replaced by sphalerite and jamesonite. (C) Pyrite crystal replaced by calcite and jamesonite. (D) Disseminated galena in stibnite and sphalerite. Abbreviations: Py = Pyrite; Sp = Sphalerite; Jam = Jamesonite; Sti = Stibnite; Ccp = Chalcopyrite; Gn = Galena; Cal = Calcite.

3. Sampling and analysis

Samples were collected from different mining levels in the Jianzhupo deposit, with representative examples being made into polished thin sections. Major- and trace-element compositions of sphalerite, jamesonite, and stibnite were determined by LA–ICP–MS at the Institute of Geochemistry, Chinese Academy of Sciences, Guangxi Province, China, using Agilent 7700x ICP–MS (Agilent technologies, USA) and New Wave UP213 LA (New Wave Research, UK) systems. Instrument settings were as described by Wei et al. (2021). Standards GSE-1G and GSD-1G were used as external standards in quantitative calibration, and results were corrected using the sulfide standard MASS-1 (Wei et al., 2021; Zhou et al., 2022). Uncertainties for most elements were < 10%, based on comparison with reference values. Concentrations of the following were determined: ^{23}Na, ^{25}Mg, ^{27}Al, ^{29}Si, ^{45}Sc, ^{49}Ti, ^{51}V, ^{53}Cr, ^{55}Mn, ^{57}Fe, ^{59}Co, ^{60}Ni, ^{65}Cu, ^{66}Zn, ^{71}Ga, ^{72}Ge, ^{74}Ge, ^{75}As, ^{77}Se, ^{90}Zr, ^{93}Nb, ^{95}Mo, ^{107}Ag, ^{109}Ag, ^{111}Cd, ^{113}In, ^{115}In, ^{118}Sn, ^{121}Sb, ^{125}Te, ^{178}Hf, ^{181}Ta, ^{184}W, ^{185}Re, ^{197}Au, ^{205}Tl, ^{208}Pb, and ^{209}Bi.

4. Results

A total of 76 LA points were used for trace-element analysis: 40 in sphalerite, 29 in jamesonite, and 7 in stibnite. Major- and trace-element compositions are listed in Electronic Appendix Table S1, 2, 3.

The sphalerite samples are enriched in Mn, Fe, Cu, Cd, and Sn, with mean contents of 923, 38,630, 2,811, 7,473, and 3,703 ppm, respectively. Jamesonite is enriched in Mn, Cu, Zn, As, Ag, Cd, and Sn, with mean contents of 1,381, 1,569, 490, 217, 596, 649, and 350 ppm, respectively. Stibnite is enriched in Cu, Zn, As, and Pb, with mean contents of 212, 434, 296, and 909 ppm, respectively.

5. Discussion

5.1. Trace-element substitution mechanisms in sphalerite

Trace elements in sphalerite occur mainly in solid solution, as nanoparticles, or as mineral micro-inclusions (Cook et al., 2009; Li et al., 2020; Hu et al., 2021; Liu et al., 2022). The occurrence forms of trace elements can effectively be judged by LA–ICP–MS signal fluctuations in time-resolved depth profiles. A 'flat' signal profile commonly indicates a solid solution or evenly distributed nanoparticles (Ye et al., 2011; Gregory et al., 2014; Hu et al., 2020), while strong signal fluctuations indicate mineral micro-inclusions or an uneven distributions of nanoparticles (Cook et al., 2009; Ye et al., 2011; Ye et al., 2016; Zhuang et al., 2019).

Signals for Zn, Fe, Mn, Sn, Cu, and Cd were flat (Fig. 4A, B), indicating that these elements are present as solid solution or evenly distributed nanoparticles. Signals of In, Ag, Ga, Pb, Sb displayed little fluctuation (Fig. 4C, D), implying solid-solution, nanoparticles, and micro-inclusions. As signal fluctuated strongly (Fig. 4D), indicating its occurrence in micro-inclusions or non-uniform nanoparticles.

In the sphalerite, Zn and Fe contents are negatively correlated (Fig. 5A), implying that Fe may directly substitute for Zn. The Mn content is negatively correlated with Fe and Cd contents (Fig. 5B, C), implying that Mn inhibits Fe and Cd substitution. The Fe^{2+}, Mn^{2+}, and Cd^{2+} have similar ionic radii of 0.63, 0.66, and 0.78 × 10^{-10} m,

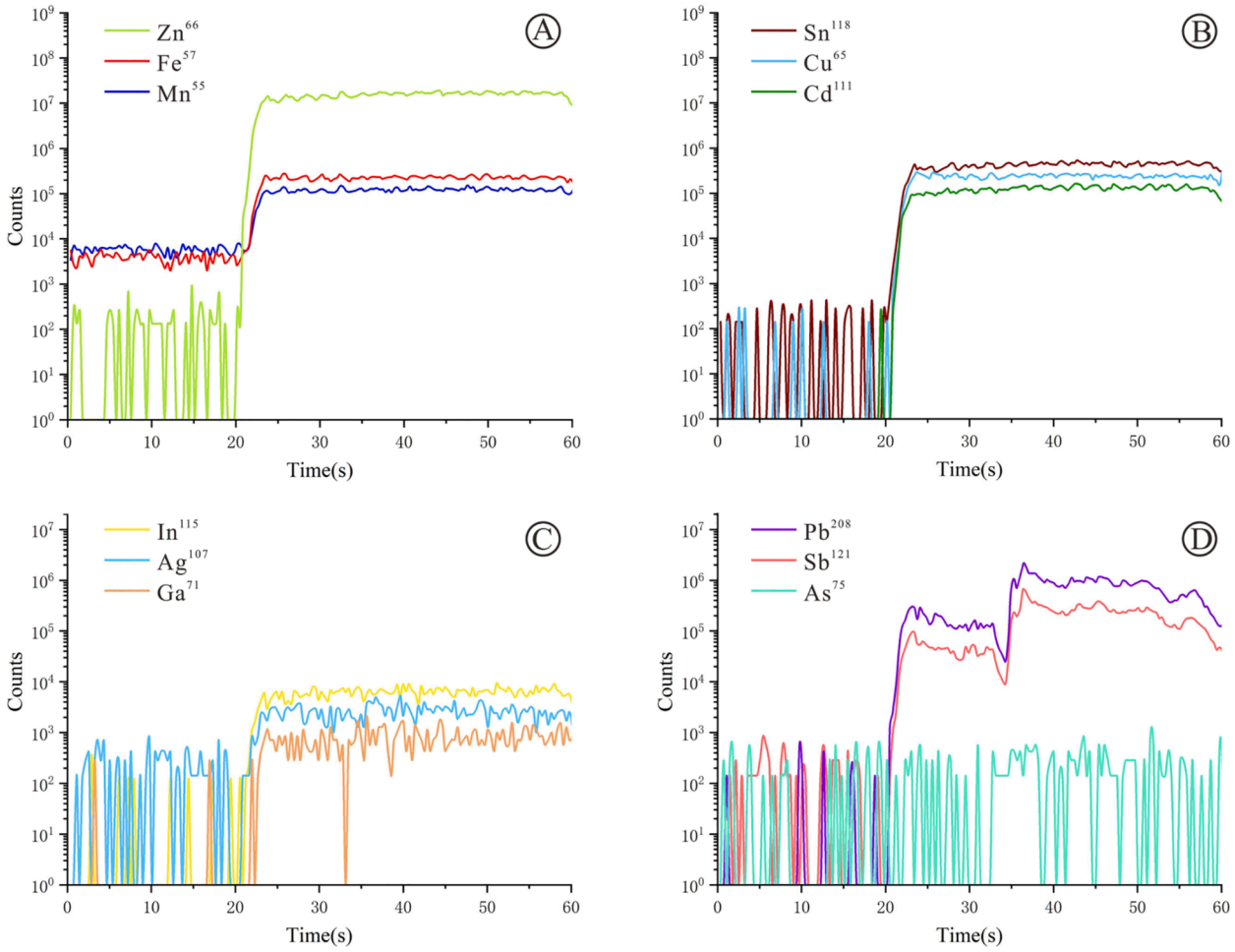

Fig. 4. Representative LA-ICP-MS time-resolved depth profiles for sphalerite.

respectively. So, these elements may directly substitute for Zn in the sphalerite lattice (Zn ↔ Fe, Cd, Mn) (Cook et al., 2009; Ye et al., 2011; Belissont et al., 2014, 2016; Hu et al., 2021; Liu et al., 2022). Due to their relatively low contents, Cd and Mn show no significant negatively correlation with Zn (Fig. 5D–F).

The charges and ionic radii of Cu, Pb, Sb, As, Ag, and Sn may differ from those of Zn, and these elements commonly occur as coupled substitutes in sphalerite (Cook et al., 2009, 2012; Ye et al., 2011; Makovicky and Topa, 2015). Cu, Sn, and Ga contents are positively correlated (Fig. 5G–I), suggesting likely substitution mechanisms of $4Zn^{2+} \leftrightarrow 2Cu^{+} + Ga^{3+} + Sn^{3+}$ or $2Zn^{2+} \leftrightarrow Cu^{+} + Ga^{3+}$ (Zhuang et al., 2019; Liu et al., 2022). Sn is strongly correlated with Cu and Ag (Fig. 5G, J), with a possible substitution mechanism of $2Zn^{2+} \leftrightarrow Sn^{3+} + (Cu^{+}, Ag^{+})$ (Cook et al., 2009). Thus, the possible substitution mechanisms are $2Zn^{2+} \leftrightarrow Ag^{+} + Ga^{3+}$ and $2Zn^{2+} \leftrightarrow 2Ag^{+} + Cu^{2+} + \square$ (vacancy) (Fig. 5K, L). The As content is positively correlated with Pb and Sb contents (Fig. 5M, N,). Based on the possible substitution mechanisms suggested by Zhuang et al. (2019) and Makovicky et al. (2015), we conclude that As substitution may occur through $4Zn^{2+} \leftrightarrow Pb^{2+} + 2As^{3+} + \square$ and $3Zn^{2+} \leftrightarrow Sb^{3+} + As^{3+} + \square$. There is a strong positive correlation between Pb and Sb (Fig. 5O), with similar signal profiles (Fig. 4D). Sphalerite Pb and Sb contents vary greatly, with respective ranges of 0–16,411 and 1–7705 ppm. Thus, Pb and Sb in sphalerite may occur as jamesonite micro-inclusions (Fig. 3A, B).

5.2. Distribution of trace elements in sphalerite color zones

Sphalerite color is likely controlled mainly by Fe content, with dark sphalerite commonly having higher Fe contents than pale sphalerite (Belissont et al., 2014; Wen et al., 2019; Hu et al., 2020; Wei et al., 2021). The LA–ICP–MS analyses indicate that Fe has the highest concentration of all trace elements in sphalerite (Table 1), and Fe increases from pale color to brown zones, with median values for pale, pale-yellow, and brown zones of 23,124, 28,022, and 34,256 ppm, whereas the median Zn contents decrease (633,558, 628,329, and 604,905 ppm, respectively; Fig. 6A, B). Zn and Fe contents have a strong negative correlation (Fig. 6B). Trends in Sn, Cu, Sb, Ga, and Ag contents are similar to that of Fe (Fig. 6A, D), and concentrations of these elements increase from dark to pale sphalerite. with mean values for pale, pale-yellow, and brown zones respectively as follows: Sn, 109, 276, and 10,092 ppm; Cu, 101, 265, and 7,667 ppm; Sb, 16, 29, and 228 ppm; Ga, 3.05, 3.40, and 12.77 ppm; and Ag, 2.40, 3.82, and 31.32 ppm (Table 1). There is no obvious correlation of Cd, Mn, As, In, or Pb contents with sphalerite color (Fig. 6A, C). Although variations of Sn, Cu, Sb, Ga, and Ag contents between sphalerite color zones are similar to that of Fe content, Fe is likely the dominant factor controlling sphalerite color due to its relatively high content.

5.3. Trace elements in jamesonite and stibnite

In jamesonite, signal profiles for Mn, Cu, Zn, As, Ag, Cd, Sn, and In are relatively flat in the time-resolved depth profiles (Fig. 7A–D), indicating that these elements occur mainly in solid-solution form or as evenly distributed nanoparticles (Ye et al., 2011; Gregory et al., 2014; Hu et al., 2020), while the profile for Tl show little fluctuation, implying solid-solution, nanoparticle, and micro-inclusion forms (Cook et al.,

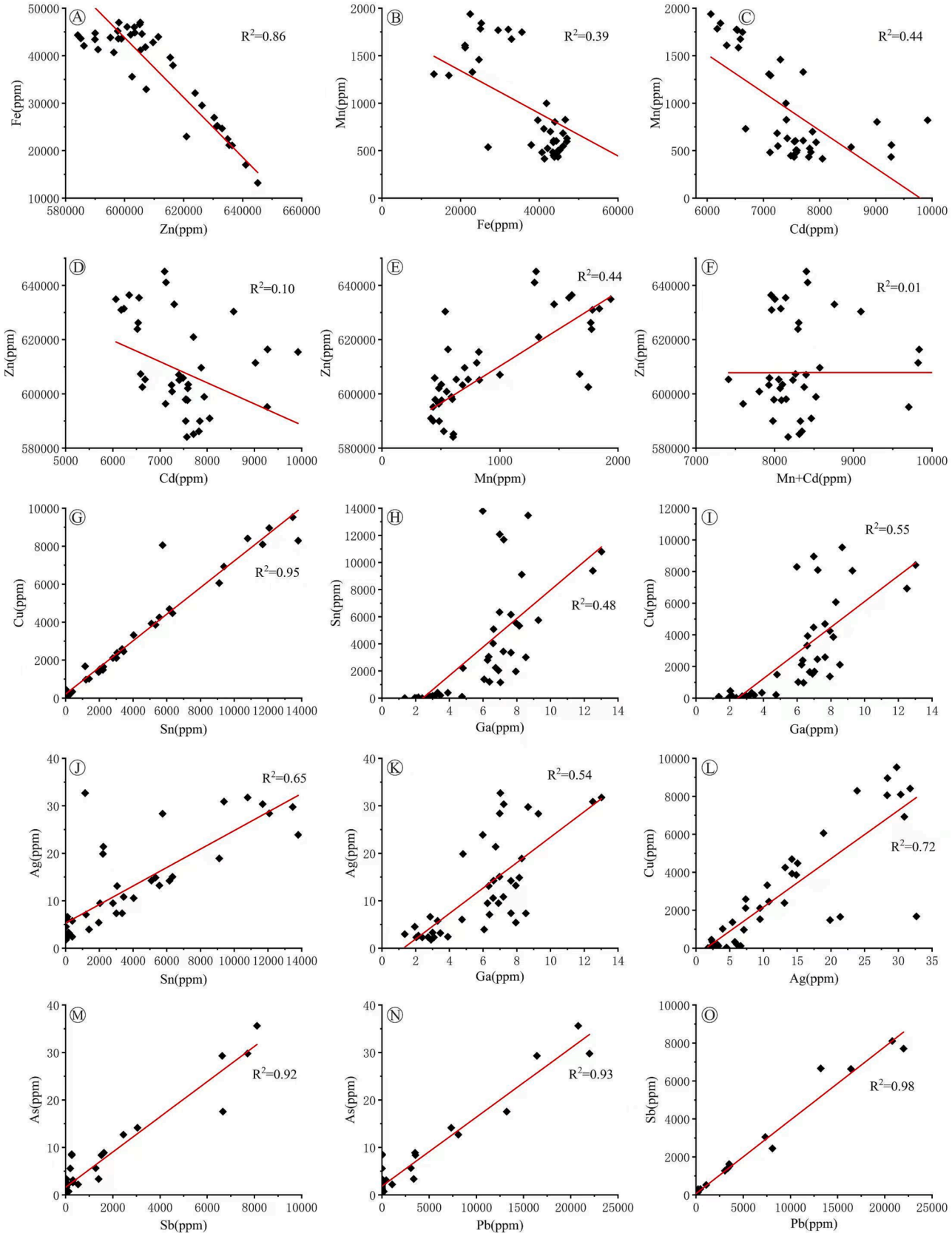

Fig. 5. Correlation plots of sphalerite: (A) Fe vs. Zn, (B) Mn vs. Fe, (C) Mn vs. Cd, (D) Zn vs. Cd, (E) Zn vs. Mn, (F) Zn vs. Mn + Cd, (G) Cu vs. Sn, (H) Sn vs. Ga, (I) Cu vs. Ga, (J) Ag vs. Sn, (K) Ag vs. Ga, (L) Cu vs. Ag, (M) As vs. Sb, (N) As vs. Pb, (O) Sb vs. Pb.

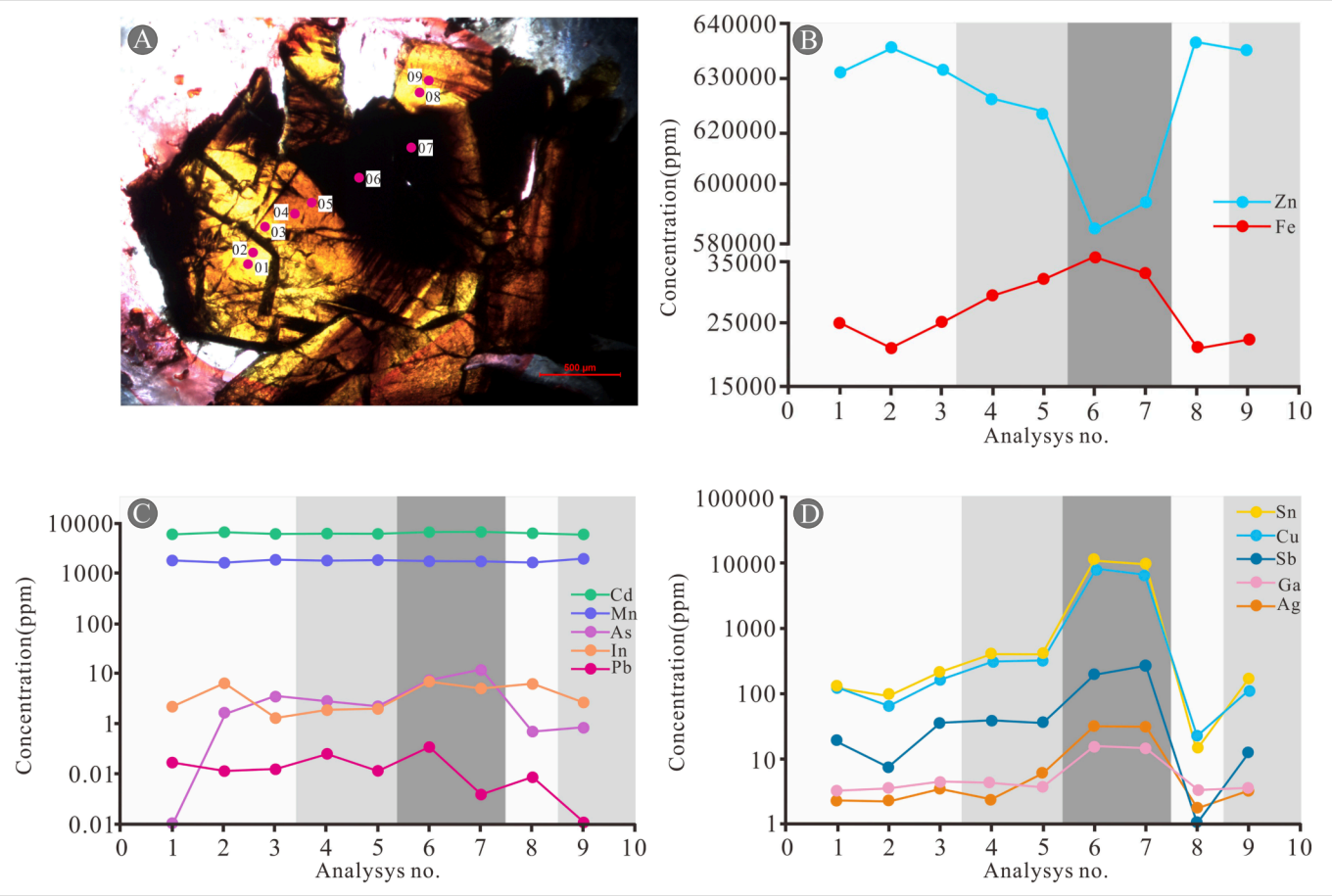

Fig. 6. Image and trace element concentrations of the color zoned sphalerite.

Table 1
LA-ICP-MS data for the three colour zones of sphalerite (ppm).

		Mn	Fe	Cu	Zn	As	Ag	Cd	In	Sn	Sb	Pb	Ga
Light zones	Max	1842	25,245	188	636,434	2.53	3.19	6555	6.09	207	36	0.16	3.46
	Min	1584	21,091	17	630,947	0.00	1.76	6177	1.23	15	1	0.08	2.74
	Mean	1705	23,124	101	633,558	1.07	2.40	6328	3.84	109	16	0.12	3.05
	S.D.	127	2316	72	2782	1.10	0.59	167	2.55	79	15	0.03	0.31
Pale-yellow bands	Max	1938	32,116	340	634,904	2.03	5.76	6536	2.47	344	38	0.23	3.91
	Min	1769	22,426	121	623,876	0.57	2.41	6064	1.78	141	12	0.00	3.00
	Mean	1828	28,022	265	628,329	1.41	3.82	6373	2.07	276	29	0.11	3.40
	S.D.	96	5016	125	5812	0.75	1.74	268	0.36	117	14	0.12	0.46
Brown cores	Max	1748	35,589	8409	607,301	8.39	31.74	6626	7.08	10,793	261	0.34	13.02
	Min	1675	32,923	6924	602,508	5.57	30.89	6588	4.71	9391	196	0.04	12.51
	Mean	1712	34,256	7667	604,905	6.98	31.32	6607	5.90	10,092	228	0.19	12.77
	S.D.	52	1885	1050	3389	1.99	0.60	27	1.68	992	46	0.21	0.36

2009; Ye et al., 2011; Ye et al., 2016; Zhuang et al., 2019). In stibnite, Cu, Pb, and As similarly occur mainly in solid-solution or evenly distributed nanoparticle forms; Zn and Ag in solid-solution, nanoparticle, and micro-inclusion forms; and Cd, Sn, and Tl, which have strongly fluctuating signal profiles that may be caused by their low concentrations. (Fig. 7E, F (Cook et al., 2009; Ye et al., 2011; Ye et al., 2016; Zhuang et al., 2019).

Bivalent Mn, Fe, Cd ions have radii similar to that of Zn^{2+} and are able to directly replace Zn in the sphalerite lattice (Cook et al., 2009; Ye et al., 2011; Zhuang et al., 2019; Hu et al., 2021; Liu et al., 2022; Zhou et al., 2022). Furthermore, Zn content is positively correlated with Mn and Cd contents, suggesting that Mn, Cd, and Zn may replace Fe in the jamesonite lattice according to $2Fe^{2+} \leftrightarrow Zn^{2+} + Cd^{2+}$ or $2Fe^{2+} \leftrightarrow Zn^{2+} + Mn^{2+}$ (Fig. 8A, B). In stibnite, the strong positive correlation of Pb content with Cu and As contents and their flat time-resolved depth profiles (Fig. 7E, F and 8C, D) indicate that these elements enter stibnite through coupled substitution mechanisms of $Cu^{+}+Pb^{2+} \leftrightarrow Sb^{3+}+ \square$ and/or $3Pb^{2+}+As^{3+} \leftrightarrow 3Sb^{3+}+ \square$.

5.4. Substitution of Cd in jamesonite

Cd and Zn are in the same group in the periodic table and therefore have similar chemical properties, with Cd usually occurring in sphalerite through isomorphic replacement of Zn (Tu et al., 2004; Cook et al., 2009). In the present study, measured sphalerite Zn and Cd contents are ~ 620,960 and ~ 7707 ppm, respectively, with a mean Zn/Cd ratio of 83. Zn and Cd contents of jamesonite were relatively stable, with means of 490 and 649 ppm, respectively, and a mean Zn/Cd ratio of 0.76, much

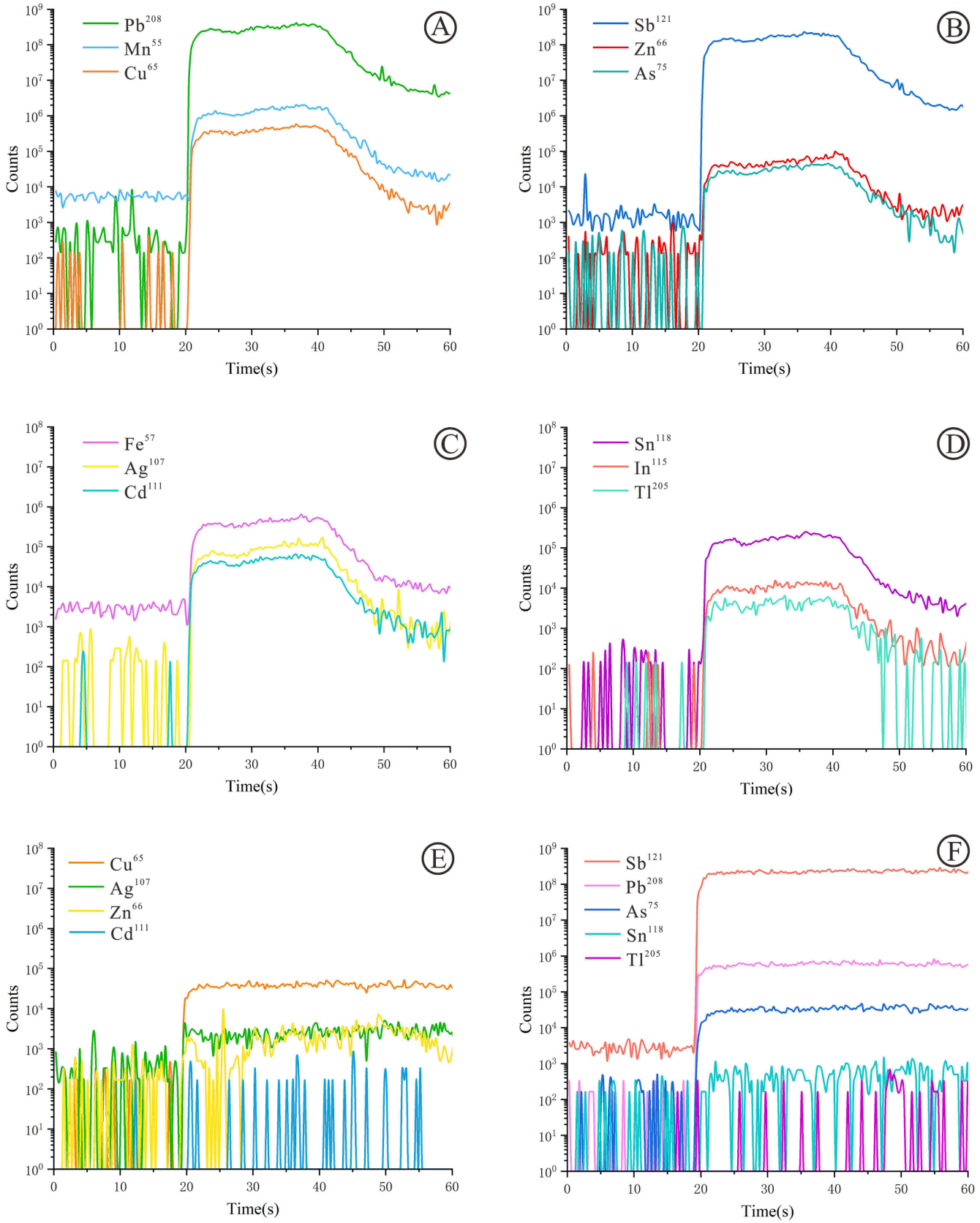

Fig. 7. Representative LA-ICP-MS time-resolved depth profiles for jamesonite (A to D) and stibnite (E, F).

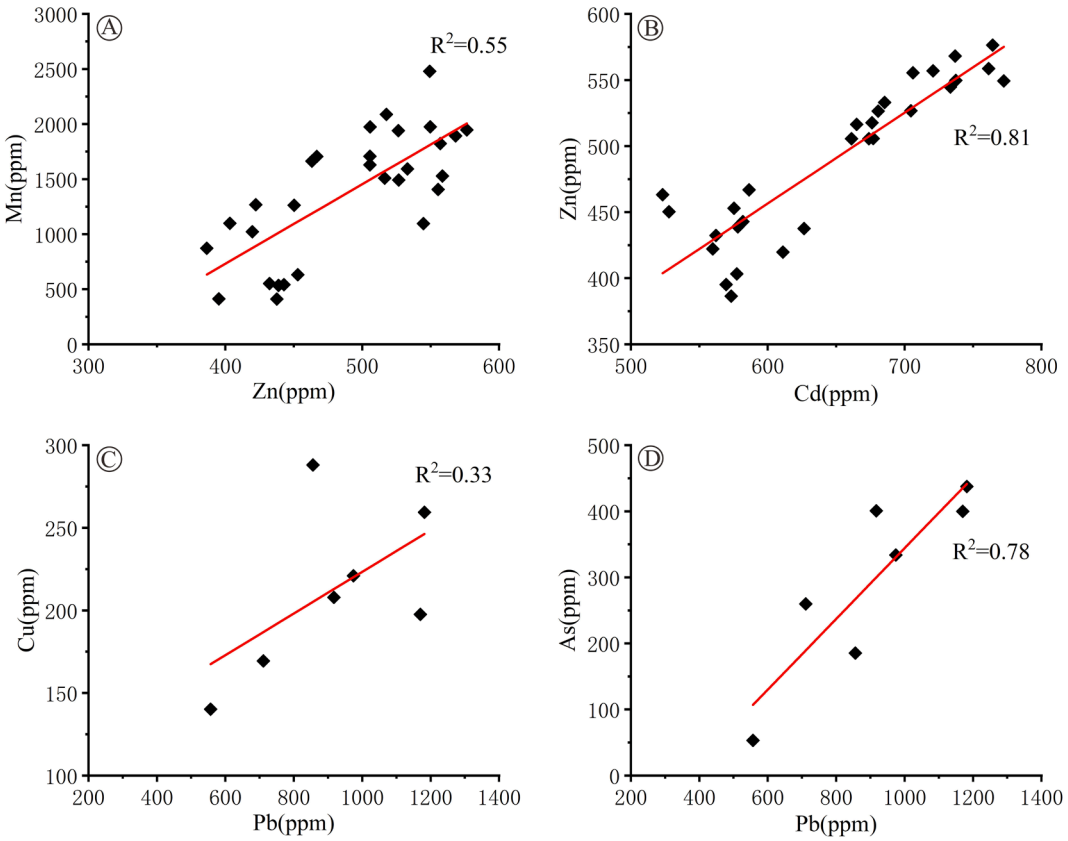

Fig. 8. Correlation plots of jamesonite (A, B) and stibnite (C, D): (A) Mn vs. Zn, (B) Zn vs. Cd, (C) Cu vs. Pb, (D) As vs. Pb.

lower than that of sphalerite. Jamesonite Zn, Cd, and Fe contents are stable from crystal margin to core (Fig. 9), implying that these elements are not affected by surrounding sphalerite. Cd in jamesonite is thus not derived from sphalerite micro-inclusions; rather, its flat time-resolved depth profiles (Fig. 7C) suggest that Cd replaces an ion in the jamesonite lattice.

The chemical formula of jamesonite is $Pb_4FeSb_6S_{14}$, comprising Pb^{2+}, Fe^{2+}, Sb^{3+}, and S^{2-}. The valence states of Fe and Pb are the same as the common Cd^{2+} state, so Cd is more likely to replace these ions. The coordination number of Sb^{3+} in both jamesonite and stibnite is three, but the latter contains no Cd, precluding replacement of Sb by Cd in jamesonite (Table S3; Zhao et al., 2015). In the jamesonite crystal lattice, the coordination number of Pb is six. The Pb valence state in galena is + 2 and its coordination number six, as for jamesonite, but galena contains no Cd, so it is unlikely that Cd replaces Pb in jamesonite (Zhao et al., 2015). In jamesonite, the coordination number of Fe is four while in pyrite it is six, and pyrite contains no Cd (Wang et al., 2019). With a coordination number of four, the ionic radii of Zn^{2+}, Cd^{2+}, and Fe^{2+} are

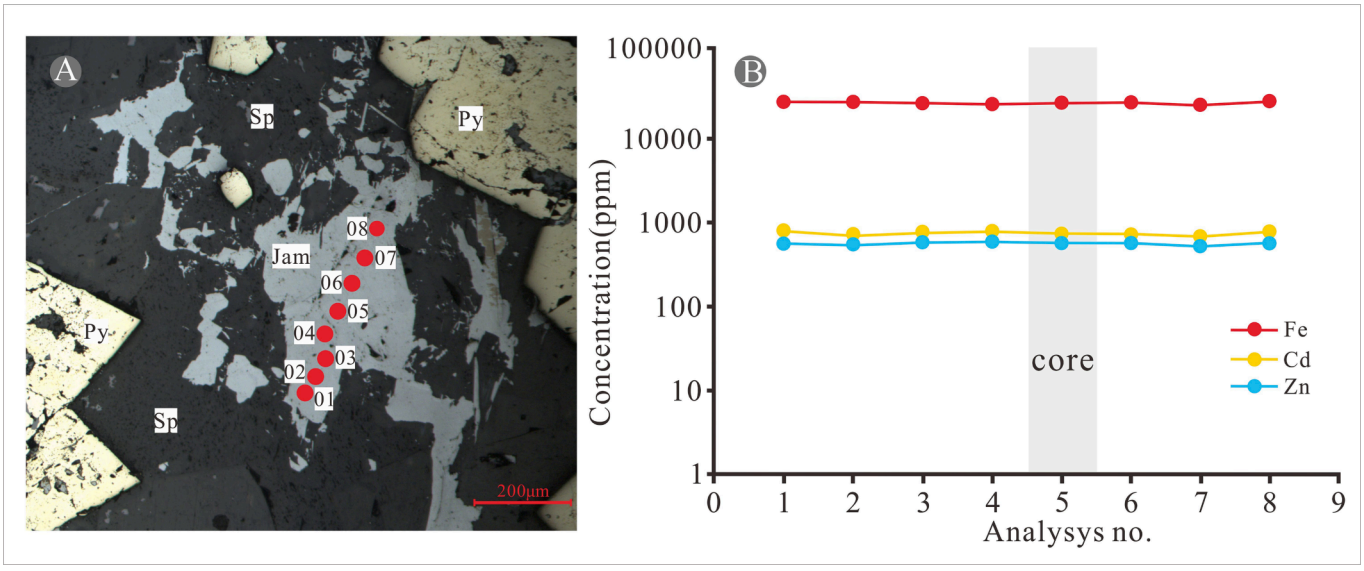

Fig. 9. Image and trace element concentrations of jamesonite.

similar at 0.6, 0.78, and 0.63 × 10^{-10} m, respectively, so they may substitute for each other (Zhou et al., 2012). It has been shown previously that Cd and Fe directly replace Zn in the sphalerite lattice (Cook et al., 2009; Ye et al., 2011; Hu et al., 2021; Liu et al., 2022; Belissont et al., 2014, 2016) and, similarly, Cd and Zn may replace Fe in jamesonite. The Cd content has a strong positive correlation with Zn content in the jamesonite (Fig. 8B), so we speculate that Cd and Zn occur in jamesonite through a coupled substitution mechanism of $2Fe^{2+} \leftrightarrow Zn^{2+} + Cd^{2+}$, but this requires further verification.

5.5. Implications

The mineralization environment and metal sources of sphalerite may be elucidated through analysis of its trace-element composition (Cook et al., 2009; Ye et al., 2011; Belissont et al., 2014; Hu et al., 2020; Li et al., 2020; Liu et al., 2022). For example, magmatic deposits have relatively high contents of Fe, In, and Mn (Ye et al., 2011; Murakami and Ishihara, 2013; Wei et al., 2018; Liu et al., 2022), while lower-temperature deposits are enriched in As, Cd, Ge, Tl, Ga, and Se (Cook et al., 2009; Ye et al., 2011; Yuan et al., 2018; Zhuang et al., 2019). Sphalerite of the Jianzhupo deposit is enriched in Mn, Fe, Cu, Cd, and Sn; depleted in Ga, As, Ag, and In; and free of Ge, Tl, and Se. Its trace-element composition is similar to that of magmatic deposits, and its ore-forming fluids may be magmatic–hydrothermal.

Distributions of trace elements in different deposits are summarized in binary plots in Fig. 10. Mineralization conditions of a deposit can be determined through comparison with typical deposits (Ye et al., 2011; Li et al., 2020; Liu et al., 2020; Hu et al., 2021). Here, most sphalerite samples plot in the VMS and Skarn deposit fields (Fig. 10), so the Jianzhupo deposit is likely of magmatic–hydrothermal origin.

Cd and Zn have similar geochemical properties and follow similar geological evolutions, especially when combined with S (Tu et al., 2004; Metz and Trefry, 2000). The sources of ore-forming fluids have been intensively studied through comparison of mineral Zn/Cd ratios (e.g., Wen et al., 2016; Metz and Trefry, 2000). In most previous studies, Cd contents were generally high in sphalerite and very low in other minerals, so they were limited to analyses of Zn/Cd ratios in sphalerite (Wang et al., 2016). However, jamesonite in the Jianzhupo deposit has high Cd contents, allowing elucidation of the genesis of the deposit through comparison of Zn/Cd ratios of sphalerite and jamesonite. Cd is generally enriched in low-temperature sedimentary deposits, and Zn/Cd ratios in sphalerite are high in high-temperature deposits such as the Baiyinnuoer and the Gacun deposits (mean Zn/Cd = 226 and 193, respectively), while for low-temperature deposits such as the Fule and the Dadongla deposits the mean ratios are lower at 33 and 30, respectively (Wen et al., 2016). In the present study, Zn/Cd ratios of sphalerite in the Jianzhupo deposit range from 64 to 105 (mean 83), similar to the Dongpo orefield (59–116, mean 83) (Fig. 11A; Li and Peng, 1989). The Dongpo orefield has a medium-temperature hydrothermal type source, with ore-forming fluids derived mainly from igneous rocks and sediments (Liu, 2003). The Zn/Cd ratios reported for the Jianzhupo orefield are slightly lower than those of the Mangchang (110–115, mean 112) and Dachang (108–159, mean 130) orefields (Fig. 11A; Wei et al., 2017; Tang, 2017). Both these orefields include magmatic-rock exposures, with ore-forming fluids are closely related to magmatic–hydrothermal (Wang et al., 2004; Pi et al., 2015; Tang, 2017). We speculate that the slightly lower Zn/Cd ratios of sphalerite in the Jianzhupo deposit may be caused by magmatic–hydrothermal fluids mixing with basin water during mineralization. Yang et al. (2023) conducted Cd isotopic analysis of sulfides in the Jianzhupo deposit, and the results showed that the metals of sphalerite and jamesonite were derived from igneous rocks and sedimentary rocks, respectively.

The Zn/Cd ratios of jamesonite in the Jianzhupo deposit range from

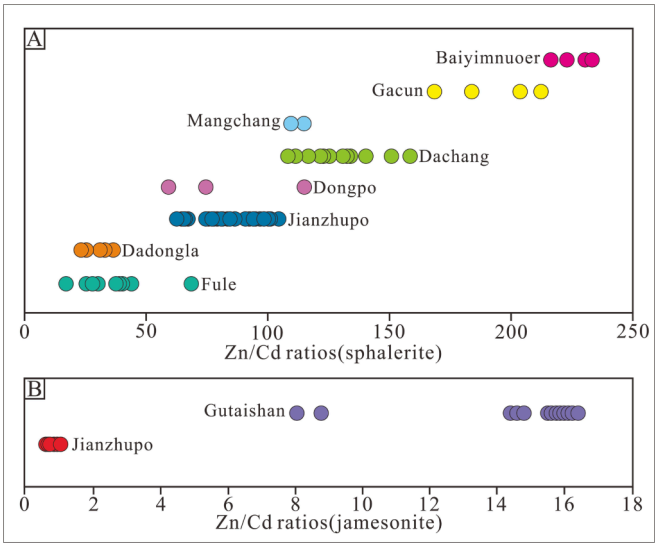

Fig. 11. Zn/Cd ratios from different types of deposits. (A) Zn/Cd ratios of sphalerite, (B) Zn/Cd ratios of jamesonite. These data are collected from Wen et al. (2016), Wang et al. (2016), Tang (2017), Wei et al. (2017) and Li (2019c).

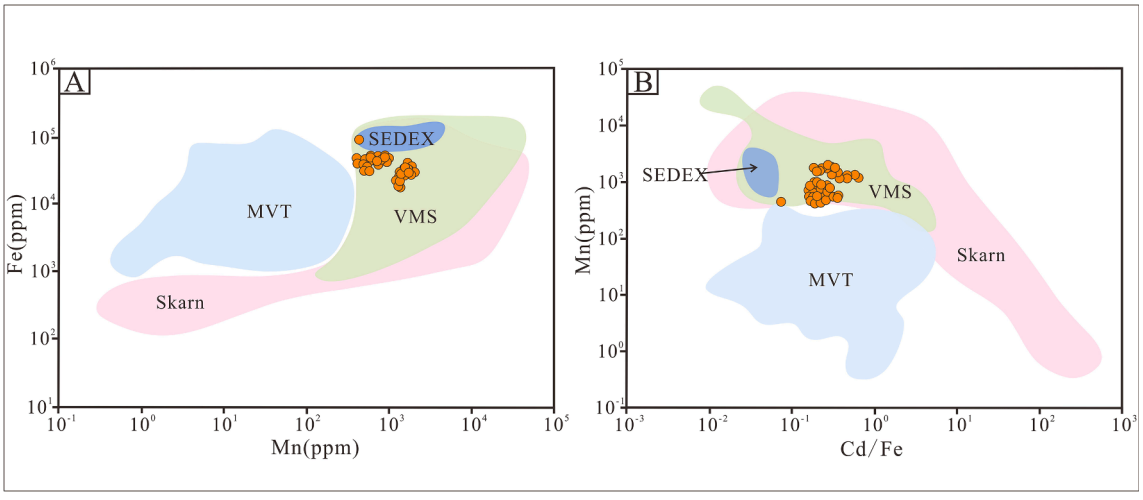

Fig. 10. Binary plots of (A) Fe vs. Mn, (B) Mn vs. Cd/Fe in sphalerite. These data are collected from Cook et al. (2009), Ye et al. (2011, 2016), George et al. (2015, 2016), Li et al. (2020) and Liu et al. (2022).

0.67 to 0.89 (mean 0.76), notably lower than values for the Gutaishan deposit, which is characterized by magmatic–hydrothermal ore-forming fluids (Fig. 11B; Li, 2019c). This may reflect a decrease in the proportion of magmatic–hydrothermal fluids during mineralization of part of the orebody with an increasing predominance of metal fluids from basin water, resulting in the formation of a high-grade jamesonite orebody in some ore sections. We conclude that ore-forming fluids of the Jianzhupo deposit are of magmatic–hydrothermal and basin-water origin.

6. Conclusions

(1) Fe, Mn, and Cd can directly substitute for Zn in sphalerite lattice (Zn ↔ Fe, Cd, Mn). Cu, Pb, Sb, As, Ag, and Sn exist in sphalerite by coupled substitution mechanisms, and the substitution mechanisms include: $4Zn^{2+} \leftrightarrow 2Cu^{+} + Ga^{3+} + Sn^{3+}$, $2Zn^{2+} \leftrightarrow Cu^{+} + Ga^{3+}$, $2Zn^{2+} \leftrightarrow Sn^{3+} + (Cu^{+}, Ag^{+})$, $2Zn^{2+} \leftrightarrow Ag^{+} + Ga^{3+}$, $2Zn^{2+} \leftrightarrow 2Ag^{+} + Cu^{2+} + \square$, $4Zn^{2+} + Pb^{2+} + 2As^{3+} + \square$ and $3Zn^{2+} \leftrightarrow Sb^{3+} + As^{3+} + \square$ (vacancy). Mn, Cd, and Zn may replace Fe in the jamesonite as $2Fe^{2+} \leftrightarrow Zn^{2+} + Cd^{2+}$ or $2Fe^{2+} \leftrightarrow Zn^{2+} + Mn^{2+}$. The coupled substitution mechanisms of Cu, Pb and As in stibnite are $Cu^{+} + Pb^{2+} \leftrightarrow Sb^{3+} + \square$ and/or $3Pb^{2+} + As^{3+} \leftrightarrow 3Sb^{3+} + \square$.

(2) In binary composition plots, most sphalerite samples plot in the VMS and Skarn deposit fields, indicating that ore-forming fluids may be of magmatic–hydrothermal origin, although Zn/Cd ratios of sphalerite and jamesonite indicate two types of ore-forming fluid in the Jianzhupo deposit: magmatic–hydrothermal and basin-water fluid.

Declaration of Competing Interest

The authors declare that they have no known competing financial interests or personal relationships that could have appeared to influence the work reported in this paper.

Data availability

Data will be made available on request.

Acknowledgments

This research was financially supported by the Technology Foundation of Guizhou Province (Grant [2019]1459), the National Natural Science Foundation of China (Grants 92162214, 41773015, U1812402, and 92162218), the Key Research and Development Program of Yunnan Province (Grant 202103AQ100003), and a special fund managed by the State Key Laboratory of Ore Deposit Geochemistry, Chinese Academy of Sciences.

Appendix A. Supplementary data

Supplementary data to this article can be found online at https://doi.org/10.1016/j.oregeorev.2023.105628.

References

Belissont, R., Boiron, M.C., Luais, B., Cathelineau, M., 2014. LA-ICP-MS analyses of minor and trace elements and bulk Ge isotopes in zoned Ge-rich sphalerites from the Noailhac–Saint-Salvy deposit (France): Insights into incorporation mechanisms and ore deposition processes. Geochim. Cosmochim. Acta 126, 518–540.

Belissont, R., Munoz, M., Boiron, M.C., Luais, B., Mathon, O., 2016. Distribution and oxidation state of Ge, Cu and Fe in sphalerite by μ-XRF and K-edge μ-XANES: insights into Ge incorporation, partitioning and isotopic fractionation. Geochim. Cosmochim. Acta 177, 298–314.

Cai, M.H., Mao, J.W., Liang, T., Franco, P., Huang, H.L., Mineralium, D., 2007. The origin of the Tongkeng-Changpo tin deposit, Dachang metal district, Guangxi, China: clues from fluid inclusions and He isotope systematics. Miner. Deposita 42, 613–626.

Cai, J.M., Xu, X.H., Li, B.H., 1995. Geochemical characteristics of inclusions in Wuxu polymetallic ore field. J. Chengdu Univ. Technol. 01, 69–77 in Chinese with English abstract.

Cai, M.H., Zhao, G.C., Zheng, Y., Wang, X.B., Guo, T.F., Liu, H., 2012. Ore-controlling Structural Styles of the Nandan- Hechi Metallogenic Belt in Northwestern Guangxi. Geol. Explor. 48 (01), 68–75 in Chinese with English abstract.

Chang, J., Li, Y.Z., Zhao, J., Cai, M.H., Hu, J.G., Peng, Z.A., 2016. Characteristics of fluid inclusions of Jianzhupo Pb- Zn deposit in Wuxu ore field of Guangxi and its geological significance. Mineral Resour. Geol. 30 (02), 270–277 in Chinese with English abstract.

Cook, N.J., Ciobanu, C.L., Pring, A., Skinner, W., Shimizu, M., Danyushevsky, L., Saini-Eidukat, B., Melcher, F., 2009. Trace and minor elements in sphalerite: A LA-ICPMS study. Geochim. Cosmochim. Acta 73 (16), 4761–4791.

Cook, N.J., Ciobanu, C.L., Brugger, J., Etschmann, B., Howard, D.L., Jonge, M.D., Ryan, C., Paterson, D., 2012. Determination of the oxidation state of Cu in substituted Cu-In-Fe-bearing sphalerite via μ-XANES spectroscopy. Am. Mineral. 97 (2–3), 476–479.

Fu, M., Kwak, T.A.P., Mernagh, T.P., 1993. Fluid inclusion studies of zoning in the Dachang tin-polymetallic ore field, People's Republic of China. Econ. Geol. 88 (2), 283–300.

George, L., Cook, N.J., Ciobanu, C.L., Wade, B.P., 2015. Trace and minor elements in galena: A reconnaissance LA-ICP-MS study. Am. Mineral. 100 (2–3), 548–569.

George, L., Cook, N.J., Ciobanu, C.L., 2016. Partitioning of trace elements in co-crystallized sphalerite–galena–chalcopyrite hydrothermal ores. Ore Geol. Rev. 77, 97–116.

Gregory, D., Meffre, S., Large, R., 2014. Comparison of metal enrichment in pyrite framboids from a metal-enriched and metal-poor estuary. Am. Mineral. 99 (4), 633–644.

Guo, J., Zhang, R., Sun, W., Ling, M., Hu, Y., Wu, K., Luo, M., Zhang, L., 2018. Genesis of tin-dominant polymetallic deposits in the Dachang district, South China: Insights from cassiterite U-Pb ages and trace element compositions. Ore Geol. Rev. 95, 863–879.

Hu, Q.F., Liu, W., An, Y.W., Ding, R.F., 2017. The Geological Geochemical Characteristics and Ore Genesis of Jian Frenzel po Pb-Zn-Sb Deposit in Hechi of Guangxi. Geol. Rev. 63 (S1) in Chinese with English abstract.

Hu, Y., Wei, C., Ye, L., Huang, Z., Danyushevsky, L., Wang, H., 2021. LA-ICP-MS sphalerite and galena trace element chemistry and mineralization-style fingerprinting for carbonate-hosted Pb-Zn deposits: Perspective from early Devonian Huodehong deposit in Yunnan, South China. Ore Geol. Rev. 136, 104253.

Hu, Y.S., Ye, L., Wei, C., Li, Z.L., Huang, Z.L., Wang, H.Y., 2020. Trace Elements in Sphalerite from the Dadongla Zn-Pb Deposit, Western Hunan-Eastern Guizhou Zn-Pb Metallogenic Belt, South China. Acta Geol. Sin.-English Ed. 94 (6), 2152–2164.

Li, W., 2019. Nature and genesis of the Gutaishan and Yuhengtang Au-Sb deposits, Xiangzhong district. China University of Geosciences, China in Chinese with English abstract.

Li, W., Cook, N.J., Ciobanu, C.L., Xie, G., Wade, B.P., Gilbert, S.E., 2019a. Trace element distributions in (Cu)-Pb-Sb sulfosalts from the Gutaishan Au-Sb deposit, South China: Implications for formation of high fineness native gold. Am. Mineral. 104 (3), 425–437.

Li, W., Cook, N.J., Xie, G.-Q., Mao, J.-W., Ciobanu, C.L., Li, J.-W., Zhang, Z.-Y., 2019b. Textures and trace element signatures of pyrite and arsenopyrite from the Gutaishan Au–Sb deposit, South China. Mineralium Deposita. 54 (4), 591–610.

Li, D.N., Peng, M.S., 1989. The typomorphic features, formation conditions and electronic structure of sphalerite. Mineral Deposits 03, 75–82 in Chinese with English abstract.

Li, W., Xie, G., Cook, N.J., Mao, J., Li, C., Ciobanu, C.L., Zhang, Z., 2021. Tracking dynamic hydrothermal processes: Textures, in-situ Sr-Nd isotopes, and trace-element analysis of scheelite from the Yangjiashan vein-type W deposit, South China. Am. Mineral. 106 (12), 1987–2002.

Li, Z.L., Ye, L., Hu, Y.S., Wei, C., Huang, Z.L., Yang, Y.L., Danyushevsky, L., 2020. Trace elements in sulfides from the Maozu Pb-Zn deposit, Yunnan Province, China: Implications for trace-element incorporation mechanisms and ore genesis. Am. Mineral. 105 (11), 1734–1751.

Liang, T., Wang, D.H., Hou, K.J., Li, H.Q., Huang, H.M., Cai, M.H., Wang, D.M., 2011. LA-MC-ICP-MS zircon U-Pb dating of Longxianggai pluton in Dachang of Guangxi and its geological significance. Acta Petrol. Sin. 27 (6), 1624–1636 in Chinese with English abstract.

Liu, D., 2003. The study on genesis and minerogenetic regulations of lead-zinc deposit in Dongpo ore field. Central South University in Chinese with English abstract.

Liu, W., An, Y.W., Hu, Q.F., Zhou, S.Y., Li, L., Tao, M.R., 2015. Characteristics of multistage mineralization in Jianzhupo Pb-Zn-Sb deposit in Wuxu, Hechi of Guangxi. Mineral Resour. Geol. 29 (02), 215–220 in Chinese with English abstract.

Liu, S., Zhang, Y.u., Ai, G., Xue, X., Li, H., Shah, S.A., Wang, N., Chen, X.i., 2022. LA-ICP-MS trace element geochemistry of sphalerite: Metallogenic constraints on the Qingshuitang Pb–Zn deposit in the Qinhang Ore Belt, South China. Ore Geol. Rev. 141, 104659.

Liu, T.T., Zhu, C.W., Wang, D.P., Zhang, S.G., Zhang, Q.B., Chen, W.Y., Wang, G.H., 2020. Genesis of the Jianzhupo Pb-Zn-Sb Polymetallic Deposit in the Wuxu Ore Field, Guangxi Province: Constraints from Sulfur Isotopes of Sulfides and Trace Elements Compositions of Sphalerites. Bull. Mineralogy, Petrology Geochemistr. 39 (3), 646–662 in Chinese with English abstract.

Makovicky, E., Topa, D., 2015. Crystal chemical formula for sartorite homologues. Mineral. Mag. 79 (1), 25–31.

Metz, S., Trefry, J.H., 2000. Chemical and mineralogical influences on concentrations of trace metals in hydrothermal fluids. Geochim. Cosmochim. Acta 64 (13), 2267–2279.

Murakami, H., Ishihara, S., 2013. Trace elements of Indium-bearing sphalerite from tin-polymetallic deposits in Bolivia, China and Japan: A femto-second LA-ICPMS study. Ore Geol. Rev. 53, 223–243.

Pi, Q.H., Hu, R.Z., Wang, D.H., Miao, B.K., Qin, X.F., Chen, H.Y., 2015. Enrichment of indium in west ore belt of Dachang orefield: Evidence from ore textures and sphalerite geochemistry. Mineral Deposits 34 (02), 379–396 in Chinese with English abstract.

Song, X.F., Lai, J.Q., Xu, J.W., Liu, X.H., Li, B., He, H.S., Wang, Y.H., Shi, J., Wang, C.F., Wen, C.H., 2022. Material Source and Genesis of the Daocaowan Sb Deposit in the Xikuangshan Ore Field: LA-ICP-MS Trace Elements and Sulfur Isotope Evidence from Stibnite. Minerals. 12 (11), 1407.

Sun, D.M., Liu, X.Z., Peng, C., Zeng, Q.S., Liu, Y.C., 1994. The application of gravity and magnetic data to the study of geological structure of the Mangchang-Dachang metallogenic belt in Guangxi and the prognosis of concealed rock bodies. Geological Publishing House. 125–143 in Chinese with English abstract.

Tang, Y.H., 2017. Ore forming mechanism of Dachang tin-polymetallic ore district: evidence from element geochemistry. China University of Geosciences (Beijing). In ChInese With English Abstract.

Tu, G.C., Gao, Z.M., Hu, R.Z., Zhang, Q., Li, C.Y., Zhao, Z.H., Zhang, B.G., 2004. The Geochemistry and Deposit-Forming Mechanism of Disperse Element. Geological Publishing House, Beijing in Chinese.

Wang, D.M., 2012. A study on the characteristic and origin of the antimony deposit in Danchi metallogenic belt. Chang'an University, Guangxi in Chinese with English abstract.

Wang, D.H., Chen, Y.C., Chen, W., Sang, H.Q., Li, H.Q., Lu, Y.F., Chen, K.L., Lin, Z.M., 2004. Dating the Dachang Giant Tin-Polymetallic Deposit in Nandan, Guangxi. Acta Geologica Sinica. (01), 132-138+146 (in Chinese with English abstract).

Wang, N.D., Fu, J.F., Wang, D.L., 2019. Crystallography and Mineralogy Course. Metallurgical Industry Press, Beijing in Chinese.

Wang, G.H., Liu, B., Kuang, A.B., 2016. Cd contents and Zn/Cd Ratios of Sphalerites and Their Geological Implications. Northwest. Geol. 49 (03), 132–140 in Chinese with English abstract.

Wei, H.L., Pi, Q.H., Yang, S.R., 2017. Enrichment Regular Research of Scattered Element Cadmium in Danchi Metallogenic Belt. Min. Eng. 15 (02), 3–6 in Chinese with English abstract.

Wei, C., Ye, L., Huang, Z.L., Gao, W., Hu, Y.S., Li, Z.L., Zhang, J.W., 2018. Ore genesis and geodynamic setting of Laochang Ag-Pb-Zn-Cu deposit, southern Sanjiang Tethys Metallogenic Belt, China: constraints from whole rock geochemistry, trace elements in sphalerite, zircon U-Pb dating and Pb isotopes. Minerals. 8 (11), 516.

Wei, C., Ye, L., Huang, Z.L., Hu, Y.S., Wang, H.Y., 2021. In situ trace elements and S isotope systematics for growth zoning in sphalerite from MVT deposits: A case study of Nayongzhi. South China. Mineralogical Magazine. 85 (3), 364–378.

Wen, H.J., Zhu, C.W., Zhang, Y.X., Cloquet, C., Fan, H.F., Fu, S.H., Reports, S., 2016. Zn/Cd ratios and cadmium isotope evidence for the classification of lead-zinc deposits. Sci. Rep. 6 (1), 25273.

Wen, H.J., Zhou, Z.B., Zhu, C.W., Luo, C.G., Wang, D.Z., Du, S.J., Li, X.F., Chen, M.H., Li, H.Y., 2019. Critical scientific issues of super-enrichment of dispersed metals. Acta Petrol. Sin. 35 (11), 3271–3291 in Chinese with English abstract.

Wu, J., Yuan, H., Gan, N., Wei, S., Liao, J., Zhang, J., Liang, H., 2020. Source characteristics of magmatic rocks and zircon U-Pb age in the Mangchang ore field, Danchi metallogenic belt. Guangxi. Acta Petrologica Sinica. 36 (5), 1586–1596.

Xiao, Z.Z., 2018. The geological characteristics and metallogenic regularity of Jianzhupo Pb-Zn-Sb deposit in Wuxu ore field. Guangxi. Mineral Resources and Geology. 32 (05), 810–815 in Chinese with English abstract.

Xiao, J.J., 2022. Geochemical characteristics of sphalerite and its genetic indication in Jian Zhu Po lead-zinc-antimony polymetallic deposit in north western Guangxi. Guangxi University. In ChInese With English Abstract.

Xiao, C.-H., Chen, Z.-L., Liu, X.-C., Wei, C.-S., Wu, Y.u., Tang, Y.-W., Wang, X.-Y., 2022. Structural Analysis, Mineralogy, and Cassiterite U-Pb Ages of the Wuxu Sb-Zn-polymetallic district, Danchi Fold-and-Thrust belt, South China. Ore Geol. Rev. 150, 105150.

Xiao, Z.Z., Tang, S.Y., Zhao, Z.Y., 2021. Enrichment regularity of main ore-forming elements in Jianzhupo mining area in Wuxu orefield, Hechi City. Guangxi. Mineral Resources and Geology. 35 (01), 15–22 in Chinese with English abstract.

Xu, W.J., Liu, W., Hu, Q.F., 2019. Geochemical characteristics and prospecting significance of Jianzhupo tin polymetallic deposit in Wuxu ore field. Guangxi. Mineral Resources and Geology. 33 (04), 573–580 in Chinese with English abstract.

Yang, Z., Zhu, C.W., Wen, H.J., Zhang, Y.X., Fan., H.F., Song, W.R., Wu, Y.Z., Zhou, C., Luais, B., 2023. Cd isotopic constraints on the sources of Zn-Sb deposits: A case study of the Jianzhupo Zn-Sb deposit, Guangxi Province, China. The Geological Society of America Bulletin. Doi: 10.1130/B36855.1.

Ye, L., Cook, N.J., Ciobanu, C.L., Liu, Y.P., Zhang, Q., Liu, T.G., Gao, W., Yang, Y.L., Danyushevskiy, L., 2011. Trace and minor elements in sphalerite from base metal deposits in South China: A LA-ICPMS study. Ore Geol. Rev. 39 (4), 188–217.

Ye, L., Li, Z.L., Hu, Y.S., Huang, Z.L., Zhou, J.X., Fan, H.F., Leonid, D., 2016. Trace elements in sulfide from the Tianbaoshan Pb–Zn deposit, Sichuan Province, China: a LA–ICPMS study. Acta Petrol. Sin. 32 (11), 3377–3393 in Chinese with English abstract.

Yuan, B., Zhang, C.Q., Yu, H.J., Yang, Y.M., Zhao, Y.X., Zhu, C.C., Ding, Q.F., Zhou, Y.B., Yang, J.C., Xu, Y., 2018. Element enrichment characteristics: Insights from element geochemistry of sphalerite in Daliangzi Pb–Zn deposit, Sichuan, Southwest China. J. Geochem. Explor. 186, 187–201.

Zhang, J., Huang, W.T., Liang, H.Y., Wu, J., Chen, X.L., 2018a. Genesis of the Jianzhupo Sb–Pb–Zn–Ag deposit and formation of an ore shoot in the Wuxu ore field, Guangxi. South China. Ore Geology Reviews. 102, 654–665.

Zhang, J., Huang, W.T., Wu, J., Liang, H.Y., Chen, L., 2018b. Characteristics of ore-forming fluids and formation of bonanza in Jianzhupo Pb-Zn-Sb polymetallic deposit within Wuxu ore field, Guangxi. South China. Geochimica. 47 (03), 257–267 in Chinese with English abstract.

Zhao, C.H., Chen, J.H., Li, Y.Q., He, Q., Wu, B.Z., 2015. Electronic structure and flotation behavior of complex mineral jamesonite. Trans. Nonferrous Met. Soc. Chin. 25 (2), 590–596.

Zhao, J.Y., Liu, X.H., 2016. Ore-controlling structural characteristics and prospecting direction in Jianzhupo Sb- Zn-Pb deposit. Guangxi. Mineral Exploration. 7 (03), 471–478 in Chinese with English abstract.

Zhao, H., Su, W.C., Shen, N.P., Xie, P., Cai, J.L., Gan, W.Z., 2018. Fluid inclusion study of the Gaofeng tin-polymetallic deposit in the Dachang ore field, Guangxi. China. Acta Petrologica Sinica 34 (12), 3553–3566 in Chinese with English abstract.

Zhou, Z., Li, H., Yonezu, K., Imai, A., Tindell, T., 2023. In-situ trace elements and sulfur isotopic analyses of stibnite: Constraints on the genesis of Sb/Sb-polymetallic deposits in southern China. J. Geochem. Explor. 247, 107177.

Zhou, C., Yang, Z., Sun, H., Koua, K.A.D., Lyu, C., 2022. LA-ICP-MS trace element analysis of sphalerite and pyrite from the Beishan Pb-Zn ore district, south China: Implications for ore genesis. Ore Geol. Rev. 150, 105128.

Zhou, G.D., Ye, X.C., Wu, N.Z., 2012. Chemical Elements Survey. Science Press, Beijing in Chinese.

Zhuang, L.L., Song, Y.C., Liu, Y.C., Fard, M., Hou, Z.Q., 2019. Major and trace elements and sulfur isotopes in two stages of sphalerite from the world-class Angouran Zn–Pb deposit, Iran: Implications for mineralization conditions and type. Ore Geol. Rev. 109, 184–200.